Supplementary Methods

Antibodies and Reagents

The following antibodies were used in western blot, immunofluorescent, immunoprecipitation, and immunohistochemical analyses: Flag (F3165; Sigma-Aldrich, St Louis, MO), hemagglutinin (11666606001; Roche Diagnostics, Indianapolis, IN), Myc (Sigma-Aldrich), PDL1 (13684; Cell Signaling Technology, Danvers, MA), PDL1 (329702; BioLegend, San Diego, CA; ab205921; Abcam, Cambridge, UK), granzyme B (ab4059; Abcam), α-tubulin (B-5-1-2; Sigma-Aldrich), GSK3B (BD Transduction Laboratories, San Diego, CA), TRAF6 (Abcam), β-actin (A2228; Sigma-Aldrich), CD8 (ab22378; Abcam), MET (8198; Cell Signaling Technology), and p-MET (3077; Cell Signaling Technology). Capmatinib was purchased from Selleck Chemicals (Houston, TX) and GSK3B substrate peptide was purchased from Millipore Sigma (Burlington, MA). Active recombinant human MET, puromycin, and staurosporine were obtained from Sigma-Aldrich. Phospho-specific antibodies against phosphorylation of GSK3B at Y56 were generated by EZBiolab (Carmel, IN).

Cell Culture, Plasmids, and Transfection

All cell lines were obtained from the ATCC (Manassas, VA), independently validated using short tandem repeat DNA fingerprinting at The University of Texas MD Anderson Cancer Center, and tested negative for mycoplasma contamination. Cells were maintained in Dulbecco's modified Eagle's medium/F12 medium or RPMI 1640 medium supplemented with 10% fetal bovine serum.

pCR-Flag-TRAF6 was kindly provided by Dr Bryant Darnay. pCGN-GSK3B-WT, pCGN-GSK3B-kinase-dead, pGEX-GSK3B, pRK5–hemagglutinin-tagged ubiquitin WT, Lys48R, and Lys63R were constructed for transient transfection as described previously.[1] A series of WT GSK3B and GSK3B mutants used for various purposes were subsequently constructed using pCMV-Flag, pGEX-6P-1, and pMX-Flag-puro vectors at *Eco*RI cloning sites. GSK3B Y56F and GSK3B P51A (PE) mutants were generated using pCMV-Flag-GSK3B as a template and QuikChange Site-Directed Mutagenesis Kit (Stratagene, La Jolla, CA). All DNA constructs were validated using enzyme digestion and DNA sequencing; detailed information about the DNA sequence is available upon request. WT TRAF6- and C70A-expressing cell lines were generated by transient transfection with DNA performed with an optimal ratio of DNA to liposomes using Lipofectamine 3000 (Invitrogen, Carlsbad, CA). For stable knockdown of MET expression and induction of MET overexpression, liver cancer cells were transfected with a pGIPZ shRNA vector (control; Thermo Fisher Scientific, Rockford, IL) and pCDH-neo vector (System Biosciences, Palo Alto, CA). The MET shRNA sequences used in knockdown experiments were as follows (5′ to 3′): CCATCCAGAATGTCATTCT (sh1) and GCATTAAAGCAGCGTATC (sh2; targeting the 3′-untranslated region). Using the pCDH-MET-Flag expression vector as a template, MET-Flag kinase mutants were generated by performing site-directed mutagenesis. For generation of stable HCC cells using retroviral infection, recombinant retroviruses were produced by cotransfecting GP293 cells (Clontech, Palo Alto, CA) with a retroviral expression plasmid and VSV-G plasmids using Lipofectamine 3000 (Invitrogen). Culture supernatants containing infectious viruses were harvested 48 hours after transfection, centrifuged to eliminate cell debris, and filtered through 0.22-mm filters. For transduction of retroviral constructs, 70% confluent HCC cells were cultured in virus-containing medium plus hexadimethrine bromide (Polybrene; Chemicon International, Temecula, CA) for 1 day to generate 70% successfully infected cells by visualizing green fluorescent protein expression. Stable clones of different constructs were subsequently selected and maintained in a culture medium with puromycin 2 μg/mL. The lentiviral-based shRNA (pGIPZ plasmids) used to knock down expression of human PDL1 was purchased from the shRNA and ORFeome Core at MD Anderson. Using a pGIPZ-shPDL1/Flag-PDL1 dual-expression construct to knock down endogenous PDL1 expression and reconstitute Flag-PDL1 simultaneously, endogenous PDL1-knockdown and WT Flag-PDL1- or 4NQ mutant (N35Q/N192Q/N200Q/N219Q)-expressing cell lines were established.[2] Twenty-four hours after transfection, the medium was changed and then collected at 24-hour intervals. The collected medium containing the lentivirus was centrifuged to eliminate cell debris and filtered through 0.45-μm filters. Cells were seeded at 50% confluence 12 hours before infection, and the medium was replaced with medium containing the lentivirus. After infection for 24 hours, the medium was replaced with fresh medium, and the infected cells were selected using puromycin 2 μg/mL (InvivoGen, San Diego, CA).

Proliferation Assay

For cell proliferation assays, control HCC cells and cells previously intervened with capmatinib or tivantinib 1 μmol/L for 48 hours were used. Three thousand cells dispensed in 100-μL aliquots were seeded in a 96-well plate, and viable cells were measured after 24, 48, and 72 hours according to the manufacturer's protocol. Cells were incubated in 10% Cell Counting Kit-8 (Dojindo Molecular Technologies, Gaithersburg, MD) and diluted in culture medium for an additional 2 hours. The absorbance at a wavelength of 450 nm was used to estimate the viable cells in each well.

Flow Cytometric Analysis

To measure cell surface PDL1 expression, single HCC cells were resuspended in phosphate buffered saline (PBS) and stained with primary antibodies according to standard protocols for flow cytometry. The cells were washed twice and then stained with secondary antibodies conjugated with allophycocyanin (Life Technologies, Carlsbad, CA). Isotype immunoglobulin G or a secondary antibody alone was used as a negative control. Stained cell samples were evaluated using a BD FACSCanto II cytometer (BD Biosciences, San

Jose, CA), and flow cytometric data were analyzed using the FlowJo software program (Ashland, OR).

T-Cell–Mediated Tumor Cell Killing Assay

To analyze T-cell–killing ability in vitro, nuclear restricted red fluorescent protein-expressing tumor cells were cocultured with activated primary human T cells or peripheral blood mononuclear cells (STEMCELL Technologies, Vancouver, BC, Canada) in the presence of a caspase 3/7 substrate (Essen BioScience, Ann Arbor, MI) in 96-well plates. T cells were activated with a CD3 antibody (100 ng/mL) and interleukin-2 (10 ng/mL). After 4 days of coculture of tumor cells and T cells in 12-well plates, wells were washed with PBS twice to remove the T cells, and the surviving tumor cells were fixed and stained with a crystal violet solution. The dried plates were scanned and quantified.

Quantitative Real-Time Polymerase Chain Reaction

HCC cells were washed twice with PBS and immediately lysed in QIAzol lysis reagent. Total RNA was extracted from HCC cells using an RNeasy Plus Mini Kit (QIAGEN, Venlo, Netherlands) according to the manufacturer's instructions and then subjected to complementary DNA synthesis by reverse transcription using a SuperScript III kit (Invitrogen). Quantitative real-time polymerase chain reaction analysis of β-actin and PDL1 was performed using iQ SYBR Green Supermix (Bio-Rad, Hercules, CA) in triplicate with a real-time polymerase chain reaction machine (iQ5; Bio-Rad) and the following primers: human PDL1, 5′-TCACTTGGTAATTCTGGGAGC-3′ (forward) and 5′-CTTTGAGTTTGTATCTTGGATGCC-3′ (reverse); β-actin, 5′-GCAAAGACCTGTACGCCAACA-3′ (forward) and 5′-TGCATCCTGTCGGCAATG-3′ (reverse). All data analyses were performed using the comparative threshold cycle method. Results were normalized according to internal control β-actin mRNA expression.

Western Blot Analysis and Immunoprecipitation

Western blot analysis of target proteins was performed as previously described.[3,4] Image acquisition and band intensity quantitation for western blotting was performed using an Odyssey infrared imaging system (LI-COR Biosciences, Lincoln, NE). For immunoprecipitation, liver cancer cells were lysed in buffer (Tris-HCl 50 mmol/L, pH 8.0, NaCl 150 mmol/L, EDTA 5 mmol/L, 0.5% Nonidet P-40) and centrifuged at 16,000 $\times$ g for 30 minutes to remove debris. Cleared lysates were subjected to immunoprecipitation with antibodies. Two micrograms of antibodies were added to lysates with 30 μL of protein A/G agarose beads. Samples of tagged lysates were incubated on a rotating wheel overnight at 4°C. Beads were collected by centrifugation at 1,000 rpm for 2 minutes at 4°C and washed 5 times with ice-cold PBS buffer. Immunocomplex samples were boiled directly in 2$\times$ sodium dodecyl sulfate (SDS)-polyacrylamide gel electrophoresis sample buffer (Tris-HCl 50 mmol/K, pH 6.8, 2% SDS, 10% glycerol, 1% β-mercaptoethanol, EDTA 12.5 mmol/L, 0.02% bromophenol blue) followed by SDS-polyacrylamide gel electrophoresis and western blot analysis.

In Vitro and In Vivo Ubiquitination Assay

For an in vitro ubiquitination assay, purified GSK3B protein was incubated with in vitro translated TRAF6 or TRAF6 C70A in the presence of a ubiquitin ligation buffer containing Tris-HCl 100 mmol/L (pH 7.4), $MgCl_2$ 5 mmol/L, NaF 2 mmol/L, okadaic acid 10 nmol/L, ATP 2 mmol/L, dithiothreitol 0.6 mmol/L, E1 60 ng, E2 300 ng, and histidine (His)-tagged ubiquitin 12 mg (Sigma-Aldrich). Reaction mixtures of these materials were incubated at 37°C for 60 minutes, and the reaction was terminated by boiling for 5 minutes with an SDS sample buffer containing dithiothreitol 0.1 mol/L. These reaction products were resolved by SDS-polyacrylamide gel electrophoresis and blotted with a His-tagged ubiquitin antibody. For in vivo ubiquitination assays, HCC cells were transfected with hemagglutinin-tagged ubiquitin, Flag-tagged WT GSK3B, or GSK3B PE and TRAF6 or TRAF6 C70A. GSK3B in HCC cells was immuno-precipitated and then blotted with antibody against ubiquitin or hemagglutinin.

Tumor-Infiltrating Lymphocyte Profiling and Tumor-Cell Analysis Using Time-of-Flight Mass Cytometry or Flow Cytometry

Excised hepatocellular tumors were digested to single cells using a gentleMACS Dissociator with a mouse Tumor Dissociation Kit (Miltenyi Biotec, Auburn, CA). Tumor-infiltrating lymphocytes and tumor cells were enriched on a Ficoll gradient (Sigma-Aldrich). For time-of-flight mass cytometric analysis, tumor-infiltrating lymphocytes and tumor cells were incubated with a mixture of metal-labeled antibodies (Supplementary Table 1) for 30 minutes at room temperature, washed twice, and incubated with Cell-ID Intercalator-^{103}Rh (Fluidigm, San Francisco, CA) overnight at 4°C. A sample of labeled tumor-infiltrating lymphocytes or tumor cells was analyzed using a time-of-flight mass cytometry 2 instrument (Fluidigm) at the Flow Cytometry and Cellular Imaging Facility at MD Anderson. For flow cytometry, cells were stained with CD3 and peridinin–chlorophyll protein, CD8 and allophycocyanin or cyanine 7, and granzyme B-Pacific Blue antibodies (BioLegend). Stained samples were analyzed using the BD FACSCanto II cytometer.

Identification of Phosphorylation Sites in HCC Cells Using Mass Spectrometry

Hep3B cells overexpressing Flag-tagged GSK3B and MET were subjected to immunoprecipitation. After protein gel electrophoresis, the gel was stained with Coomassie blue. The band corresponding to GSK3B phosphorylation by MET was excised from the gel and subjected to tryptic digestion. The band containing GSK3B was subsequently isolated

using immobilized metal affinity chromatography, and enriched phospho-peptides were analyzed using micro-liquid chromatography and tandem mass spectrometry. The peptide sequences were searched against the National Center for Biotechnology Information protein sequence database using the Mascot search engine.

In Vitro Kinase Assay and Phosphorylation Analysis

Expression of glutathione S-transferase and glutathione S-transferase–GSK3B–kinase-dead fusion proteins was induced in *Escherichia coli* BL-21 cells, and these proteins were purified using glutathione-agarose beads (17-0756-01; Amersham, Little Chalfont, UK) using a standard procedure. Purified proteins were incubated with active human recombinant MET (Sigma-Aldrich) in the presence of ATP 50 μmol/L in a kinase buffer for 30 minutes at 30°C. Reaction products were subjected to SDS-polyacrylamide gel electrophoresis and then blotted with an antibody against a target protein.

For complex immune analysis, GSK3B was immunoprecipitated from whole cell lysates by incubating total cell protein 75 μg for 2 hours with a rabbit GSK3B antibody 2 μg in the presence of protein A/G agarose beads and washed as previously described.[5] The immuno-precipitates were incubated for 45 minutes at 30°C in 4× kinase assay buffer, [γ-^{32}P] ATP 10 μCi, and synthetic peptide substrate of GSK3B 150 μmol/L, spotted onto P81 phospho-cellulose, and washed in 0.75% H_3PO_4. The activity was determined by scintillation counting. Purified GSK3B (0.2 μg; Upstate Biotechnology, Waltham, MA) was used as a positive kinase control, and a negative GSK3B substrate peptide (Calbiochem, San Diego, CA) was used to detect background phosphorylation (eg, GSK3B autophosphorylation). The resulting GSK3B activity data were obtained after the background phosphorylation was subtracted.

Yeast Two-Hybrid Assay

pGBT9, pGBT-GSK3B, and pGBT-GSK3B PE paired with pACT-TRAF6 were co-transformed into yeast Y190 cells using a Matchmaker Two-Hybrid System 2 (Clontech) according to the manufacturer's instructions. Yeast cells containing corresponding vectors were grown in tryptophan and leucine selection media for 24 hours at 30°C. For a yeast survival assay, yeast transformants at an optical density of 1.6 were resuspended in PBS. Ten-fold serially diluted yeast cells were spotted onto synthetic complete medium plates lacking tryptophan, leucine, and His with or without 3-amino-1,2,4-triazole 20 mmol/L (Sigma-Aldrich). The plates were incubated at 30°C until colonies were observed.

Clinical Tumor Samples and Follow-up

Tumor samples were collected from 268 patients with HCC who underwent surgical resection from August 2001 to November 2007 at the Fudan Liver Cancer Institute (Shanghai, People's Republic of China) for use in tissue microarrays. Patients were monitored after surgery until March 15, 2009 at the Liver Surgery Department at the Zhongshan Hospital of the Fudan University (Shanghai, People's Republic of China). The Research Ethics Committee of the Zhongshan Hospital approved the use of tumor samples. Postsurgical follow-up was conducted as previously described.[6] Overall survival was defined as the interval from tumor resection to death or last follow-up examination, and disease-free survival was defined as the interval from the date of resection to the date of tumor recurrence.

Immunohistochemistry

Tissue microarrays containing HCC patient samples were constructed as previously described.[7] Mouse liver tumor samples were obtained from tumor xenografts. Immunohistochemical staining of the samples was performed as previously described.[4] Briefly, each tissue sample was stained with specific antibodies as indicated and a biotin-conjugated secondary antibody and then incubated with an avidin-biotin-peroxidase complex. Visualization of the target protein was performed using 3-amino-9-ethylcarbazole chromogen. The samples were scored using an H-score method combining the values of immunoreaction intensity and percentage of tumor-cell staining. The final immunohistochemical score was calculated by multiplying the percentage of target protein positive cells by the intensity score. The staining intensity was ranked in 4 groups according to histologic score: high (+++), medium (++), low (+), and negative (−).

Immunofluorescence

For immunocytochemistry, HCC cells were fixed in 4% paraformaldehyde at room temperature for 15 minutes, made permeable in 5% Triton X-100 for 5 minutes, and then stained with primary antibodies. Secondary antibodies used were anti-mouse Alexa Fluor 488 or 594 dye conjugate and anti-rabbit Alexa Fluor 488 or 594 dye conjugate (Life Technologies). Nuclei were stained with 4,6-diamidino-2-phenylindole (blue; Life Technologies). After mounting, the cells were visualized using a multiphoton confocal laser-scanning microscope (LSM700; Carl Zeiss, Oberkochen, Germany).

Mouse liver tumor samples were frozen in an optimal cutting temperature block immediately after extraction. Cryostat sections of samples that were 5 μm thick were attached to saline-coated slides. The cryostat sections were fixed with 4% paraformaldehyde for 15 minutes at room temperature and blocked with a blocking solution (5% bovine serum albumin, 2% donkey serum, and PBS 0.1 mol/L) at room temperature for 30minutes. Sample sections were stained with primary antibodies overnight at 4°C followed by secondary antibodies at room temperature for 1hour. The LSM700 microscope was used for image analysis.

Animal Studies

All procedures using C3H, nonobese diabetic and severe combined immunodeficiency gamma (NOD.Cg-Prkdc^{scid}Il2rg^{tm1Wjl}/SzJ), and C57BL/6 mice (male, 6 weeks old; The Jackson Laboratory, Bar Harbor, ME, USA) were conducted under guidelines approved by the MD Anderson Institutional Animal Care and Use Committee.

Tumorigenicity assays were performed using mouse subcutaneous and orthotopic liver cancer models. For the subcutaneous tumor model, HCA-1 and Hep1-6 liver cancer cells (5×10^6) were subcutaneously injected into the right inguinal fold regions of C3H and C57BL/6 mice. For the orthotopic tumor model, subcutaneous Hep1-6 tumors were cut into cubes (1 mm^3) under aseptic conditions. Then, single cubes were inoculated into the liver parenchyma of C57BL/6 mice anesthetized using xylazine. Mice were randomly assigned to groups according to mean tumor volume. For antibody-based drug intervention, PD1 antibody 100 μg (RMP1-14; Bio X Cell, West Lebanon, NH) or rat immunoglobulin G (control; Bio X Cell) were injected intraperitoneally every 3 days 1 week after tumor-cell inoculation. For drug-based drug intervention, mice were given daily oral doses of capmatinib 10 mg/kg reconstituted in 0.5% methylcellulose and 5% dimethylacetamide[8] or tivantinib 100 mg/kg[9] formulated in tocopherol polyethylene glycol 1000 succinate (BioXtra, water-soluble vitamin E conjugate). Subcutaneous tumors were measured using a caliper, and orthotopic tumors were evaluated using high-frequency ultrasound (Vevo 2100 imaging system; FUJIFILM VisualSonics Inc, Toronto, ON, Canada) twice a week (Supplementary Figure 4*A*). Tumor volumes were calculated using the formula (length $\times$ width^2)/2. At the experimental end point, mice were killed using CO_2 exposure followed by cervical dislocation, and tumors were excised for subsequent histologic analysis or processed immediately for mass cytometric and flow cytometric analyses.

Statistical Analysis

The relation of the expression of different proteins in liver tumors was determined by Pearson correlation analysis. Statistical analysis was performed using SPSS (IBM Corporation, Armonk, NY). The level of significance was set at .05.

References

1. Lee DF, Kuo HP, Liu M, et al. KEAP1 E3 ligase-mediated downregulation of NF-kappaB signaling by targeting IKKbeta. Mol Cell 2009;36:131–140.
2. Li CW, Lim SO, Xia W, et al. Glycosylation and stabilization of programmed death ligand-1 suppresses T-cell activity. Nat Commun 2016;7:12632.
3. Lim SO, Gu JM, Kim MS, et al. Epigenetic changes induced by reactive oxygen species in hepatocellular carcinoma: methylation of the E-cadherin promoter. Gastroenterology 2008;135:2128–2140 e1-8.
4. Lee DF, Kuo HP, Chen CT, et al. IKK beta suppression of TSC1 links inflammation and tumor angiogenesis via the mTOR pathway. Cell 2007;130:440–455.
5. Singer CA, Vang S, Gerthoffer WT. Coupling of M(2) muscarinic receptors to Src activation in cultured canine colonic smooth muscle cells. Am J Physiol Gastrointest Liver Physiol 2002;282:G61–G68.
6. Sun HC, Zhang W, Qin LX, et al. Positive serum hepatitis B e antigen is associated with higher risk of early recurrence and poorer survival in patients after curative resection of hepatitis B-related hepatocellular carcinoma. J Hepatol 2007;47:684–690.
7. Zhou SL, Dai Z, Zhou ZJ, et al. Overexpression of CXCL5 mediates neutrophil infiltration and indicates poor prognosis for hepatocellular carcinoma. Hepatology 2012;56:2242–2254.
8. Liu X, Wang Q, Yang G, et al. A novel kinase inhibitor, INCB28060, blocks MET-dependent signaling, neoplastic activities, and cross-talk with EGFR and HER-3. Clin Cancer Res 2011;17:7127–7138.
9. Rimassa L, Assenat E, Peck-Radosavljevic M, et al. Second-line tivantinib (ARQ 197) vs placebo in patients (Pts) with MET-high hepatocellular carcinoma (HCC): results of the METIV-HCC phase III trial. J Clin Oncol 2017;35:4000.

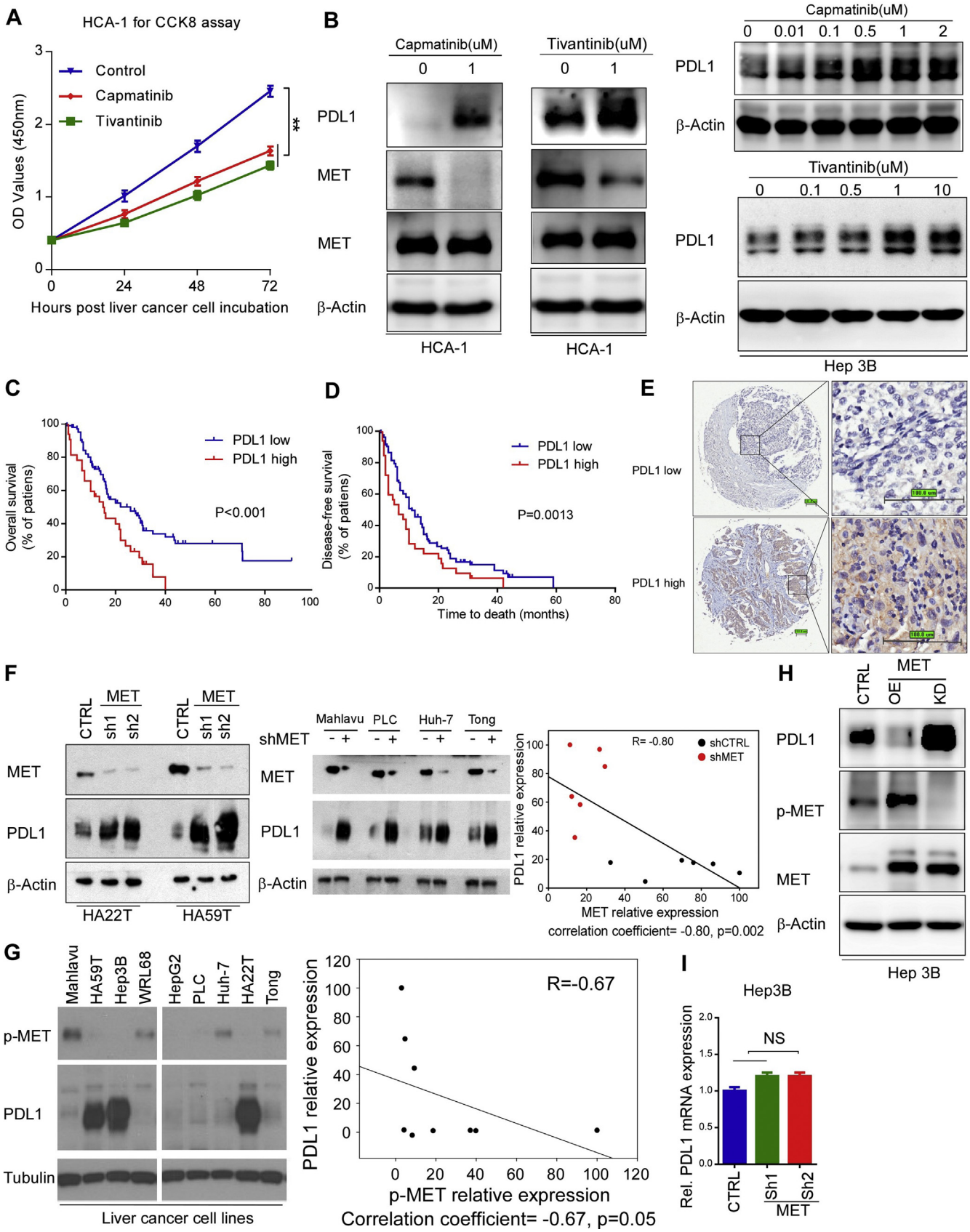
A
HCA-1 for CCK8 assay
Control
Capmatinib
Tivantinib
OD Values (450nm)
Hours post liver cancer cell incubation
B
Capmatinib(uM)
Tivantinib(uM)
PDL1
MET
β-Actin
HCA-1
Hep 3B
C
PDL1 low
PDL1 high
Overall survival (% of patiens)
P<0.001
D
Disease-free survival (% of patiens)
P=0.0013
Time to death (months)
E
PDL1 low
PDL1 high
F
CTRL
MET
sh1
sh2
shMET
Mahlavu
PLC
Huh-7
Tong
HA22T
HA59T
R= -0.80
shCTRL
shMET
PDL1 relative expression
MET relative expression
correlation coefficient= -0.80, p=0.002
G
Mahlavu
HA59T
Hep3B
WRL68
HepG2
PLC
Huh-7
HA22T
Tong
p-MET
Tubulin
Liver cancer cell lines
R=-0.67
p-MET relative expression
Correlation coefficient= -0.67, p=0.05
H
OE
KD
I
Hep3B
NS
Rel. PDL1 mRNA expression

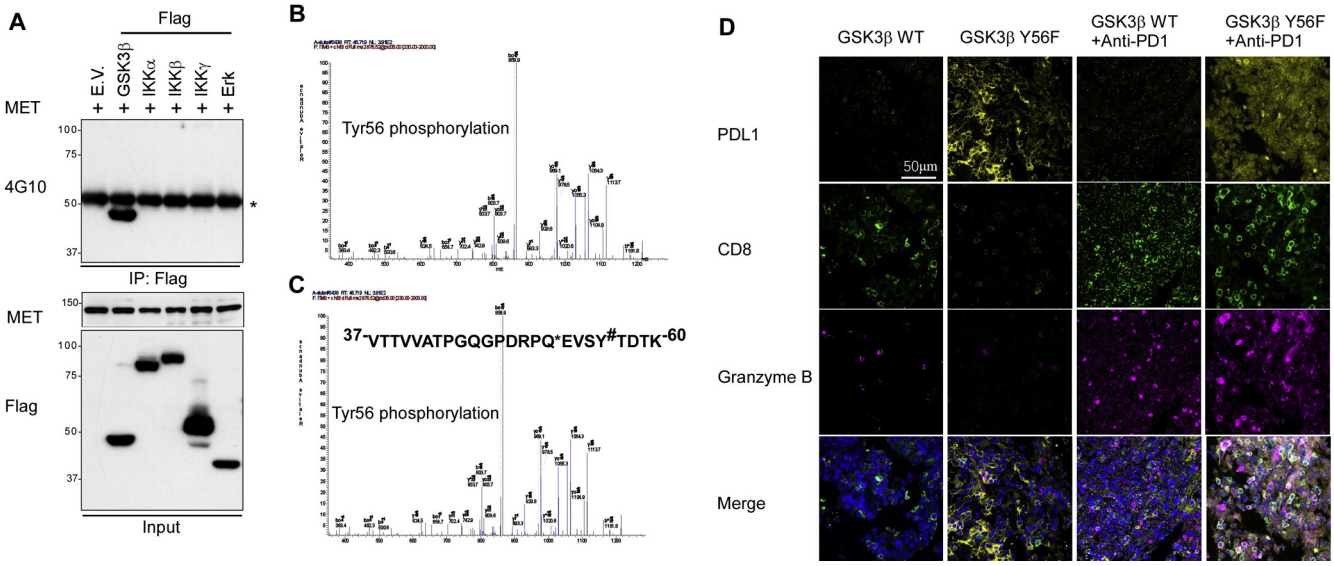

Supplementary Figure 2. MET binds to and phosphorylates GSK3B at Tyr56 to down-regulate its ubiquitination. (*A*) Hep3B cells coexpressing MET and an empty vector, Flag-GSK3B, Flag- IKKα, Flag-IKKβ, Flag-IKKγ, or Flag-ERK were immunoprecipitated with a Flag antibody. The total amount of immuno-precipitates was determined by western blotting with a phospho-tyrosine antibody (4G10) to detect phosphorylation. (*B* and *C*) Mass spectrometric analyses identifying GSK3B Y56 phosphorylation (*B*) in vivo and (*C*) in vitro. (*D*) Immunofluorescent staining of the PDL1, CD8, and granzyme B protein expression patterns in HCA-1 cells after drug intervention. ERK, extracellular signal-regulated kinase; E.V., empty vector; IKK, IκB kinase; Tyr56, Y56.

Supplementary Figure 1. MET inhibition drives PDL1 expression that correlates with poor prognosis for HCC. (*A*) Control HCA-1 cells or cells treated with capmatinib or tivantinib for 48 hours at a concentration of 1 μmol/L were subjected to a Cell Counting Kit-8 assay, and viable cells were measured after 24, 48, and 72 hours. (*B*) Immunoblot analysis of whole cell lysates derived from HCA-1 and Hep3B cell lines treated with or without the MET inhibitor capmatinib or tivantinib at the indicated concentrations for 48 hours. (*C* and *D*) Prognostic value of PDL1 expression according to Kaplan-Meier analysis of overall (*C*) and disease-free (*D*) survival in patients with HCC. (*E*) Representative HCC samples exhibiting expression of PDL1 (*yellow*) at low (*top*) and high (*bottom*) levels. Scale bars, 100 μm. (*F*) (*Left*) immunoblot of MET protein expression and PDL1 expression induced by a vector control and MET knockdown in HA22T and HA59T cells. (*Middle*) Immunoblot of MET protein expression and PDL1 expression induced by a vector control and MET knockdown in Mahlavu, PLC, Huh-7 and Tong cells. (*Right*) PDL1 quantification of western blot results from left and middle panels. Intensity of PDL1 protein was quantified using a densitometer. (*G*) (*Left*) Western blot analysis of PDL1 protein and p-MET in HCC cell lines. (*Right*) Intensity of PDL1 protein and p-MET was quantified using a densitometer. (*H*) Immunoblot of MET protein and PDL1 expression in vector control, WT MET-expressing Hep3B, and MET kinase-dead Hep3B cells. (*I*) Results of quantitative real-time polymerase chain reaction analysis of PDL1 mRNA expression in MET-knockdown Hep3B and SK-HEP-1 cells are shown. CCK8, Cell Counting Kit-8; CTRL, control; KD, kinase-dead; OE, overexpression.

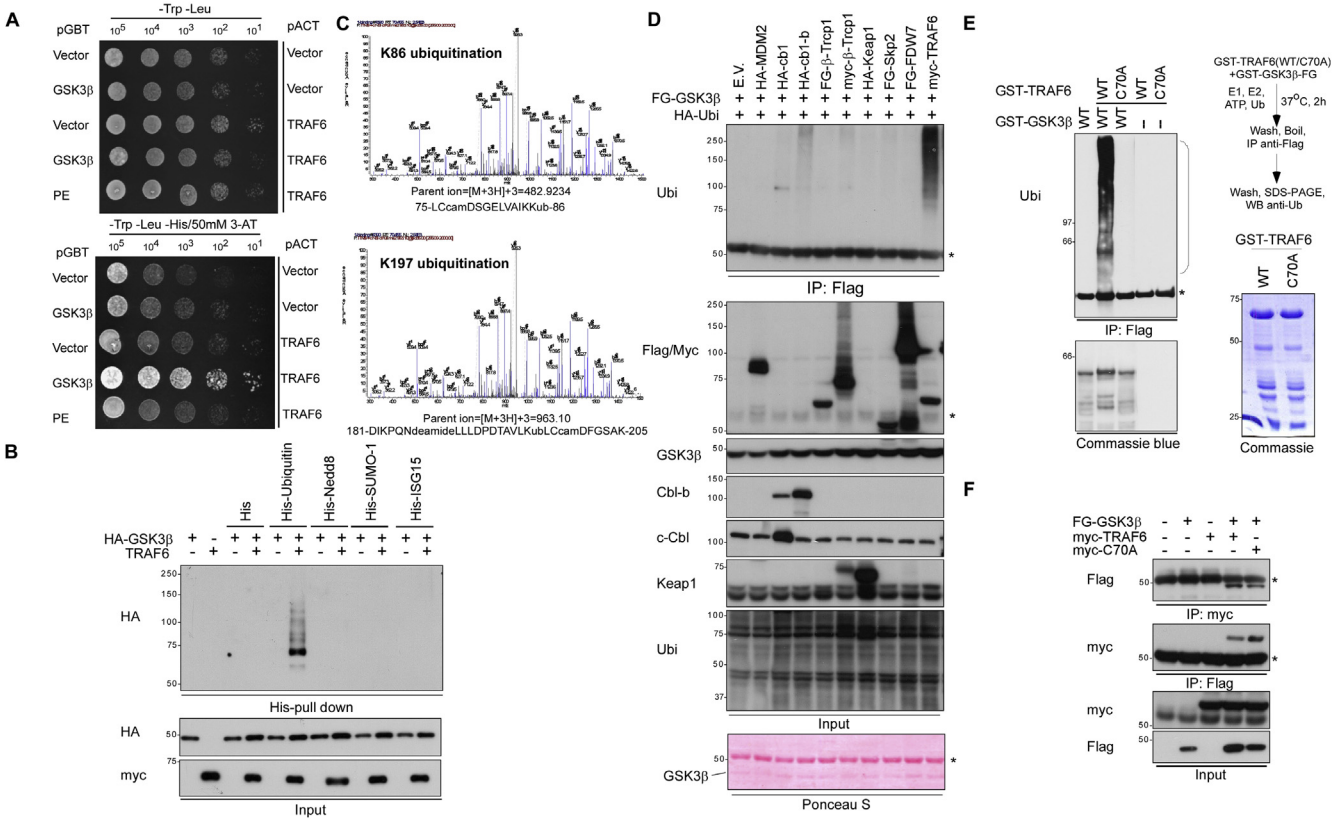

Supplementary Figure 3. MET up-regulates GSK3B activity in HCC cells by suppression of TRAF6-mediated GSK3B K63 ubiquitination. (*A*) Interaction between GSK3B and TRAF6 based on a yeast 2-hybrid assay. Yeast cells containing corresponding vectors were grown in tryptophan and leucine selection media for 24 hours at 30°C. Ten-fold serially diluted yeast cells were spotted onto synthetic complete medium plates lacking tryptophan, leucine, and histidine with or without 3-amino-1,2,4-triazole. (*B*) Hep3B cells were transfected with hemagglutinin-tagged GSK3B together with a plasmid expressing His_6, His-tagged fused ubiquitin, or Nedd8 with or without TRAF6. A covalently conjugated His-tagged ubiquitin of GSK3B in the cells was pulled down using Ni^{2+} agarose beads under denaturing conditions and analyzed using western blotting with the indicated antibodies. (*C*) Mass spectrometric analyses identifying 2 ubiquitination sites in GSK3B (K86 and K197) in Hep3B cells. (*D*) Hep3B cells were transfected with the indicated plasmids and subjected to immunoprecipitation using a Flag antibody. Ubiquitination of transfected cells was analyzed by Western blotting. (*E*) Hep3B cells were transfected with the indicated plasmids and subjected to immunoprecipitation with a Flag antibody. (*Right*) A detailed protocol for the use of in vitro ubiquitination assay is shown. Ubiquitination was analyzed by western blotting. (*F*) Immunoprecipitation of Hep3B cells transfected with the indicated plasmids. GST, glutathione S-transferase; PAGE, polyacrylamide gel electrophoresis; Ubi, ubiquitination.

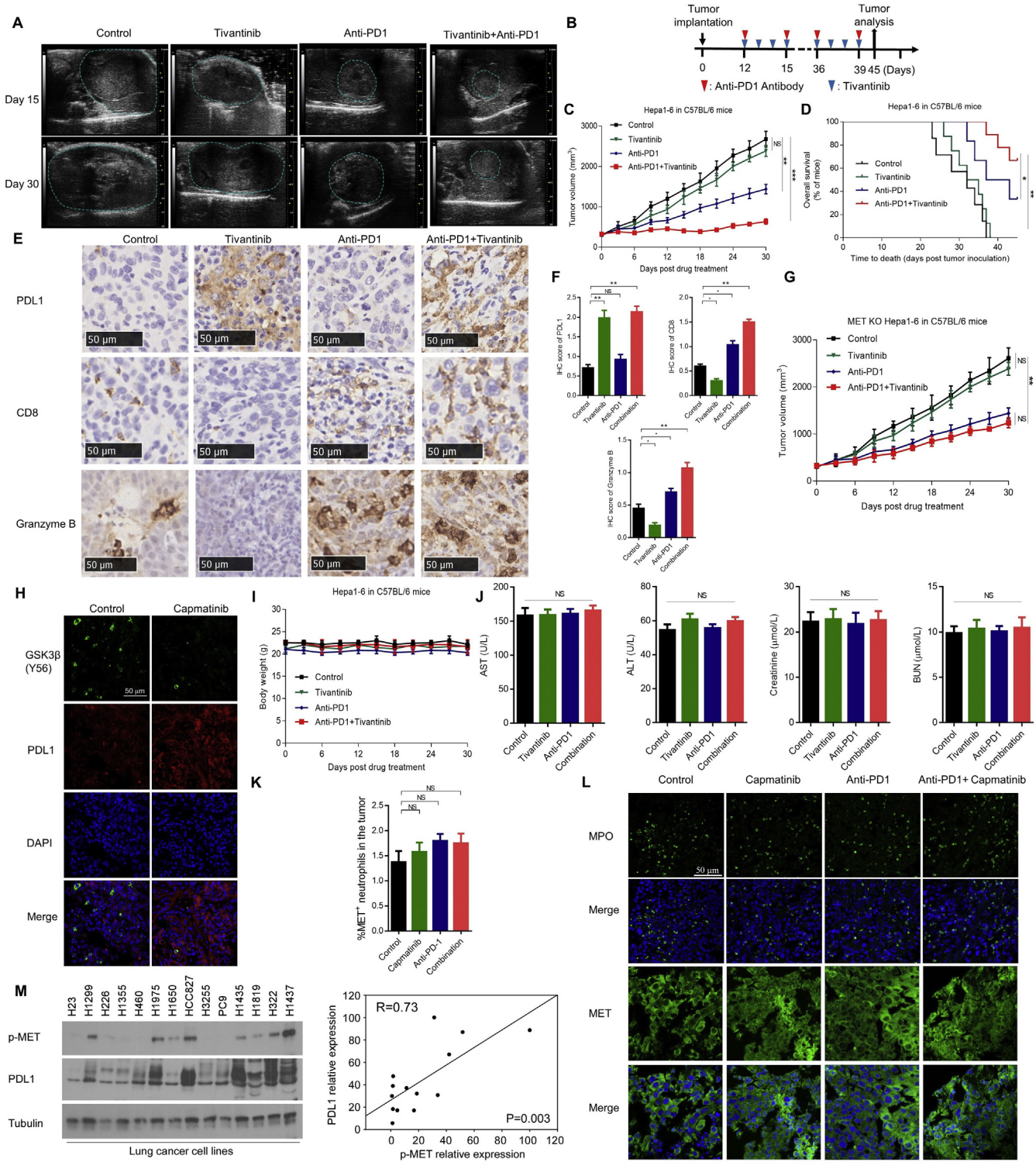
A
Control
Tivantinib
Anti-PD1
Tivantinib+Anti-PD1
Day 15
Day 30
B
Tumor implantation
Tumor analysis
0 12 15 36 39 45 (Days)
: Anti-PD1 Antibody
: Tivantinib
C
Hepa1-6 in C57BL/6 mice
Control
Tivantinib
Anti-PD1
Anti-PD1+Tivantinib
Tumor volume (mm3)
Days post drug treatment
NS
**
***
D
Hepa1-6 in C57BL/6 mice
Overall survival (% of mice)
Time to death (days post tumor inoculation)
*
**
E
Control
Tivantinib
Anti-PD1
Anti-PD1+Tivantinib
PDL1
CD8
Granzyme B
50 μm
F
IHC score of PDL1
IHC score of CD8
IHC score of Granzyme B
Control
Tivantinib
Anti-PD1
Combination
G
MET KO Hepa1-6 in C57BL/6 mice
Tumor volume (mm3)
Days post drug treatment
H
Control
Capmatinib
GSK3β (Y56)
PDL1
DAPI
Merge
I
Hepa1-6 in C57BL/6 mice
Body weight (g)
Days post drug treatment
J
AST (U/L)
ALT (U/L)
Creatinine (μmol/L)
BUN (μmol/L)
K
%MET+ neutrophils in the tumor
Control
Capmatinib
Anti-PD-1
Combination
L
Control
Capmatinib
Anti-PD1
Anti-PD1+ Capmatinib
MPO
Merge
MET
M
H23
H1299
H226
H1355
H460
H1975
H1650
HCC827
H3255
PC9
H1435
H1819
H322
H1437
p-MET
PDL1
Tubulin
Lung cancer cell lines
R=0.73
P=0.003
PDL1 relative expression
p-MET relative expression

Supplementary Table 1. Antibodies Used for Time-of-Flight Mass Cytometry Analysis (Provided by Fluidigm)

Marker	Clone	Label
Immune cell panel		
Gr-1	RB6-8C5	141Pr
CD11c	N418	142Nd
CD45	30-F11	147Sm
CD11b	M1/70	148Nd
CD19	6D5	149Sm
CD3e	145-2C11	152Sm
CD8a	53-6.7	168Er
TCRβ	H57-597	169Tm
NK1.1	PK136	170Er
CD4	RM4-5	172Yb
B220	RA3-6B2	176Yb
PD1	29F.1A12	159Tb
Tumor cell panel		
PDL1	10F.9G2	154Sm
p-NFκB	93H1	149Sm
p-STAT3	M9C6	152Sm
p-AKT	M89-61	159Tb
Ki67	B56	168Er
EpCAM	G8.8	166Er
ERK1/2	D13.14.4.E	167Er
p-Tyrosine	p-Tyr-100	144Nd
p-S6	N7-548	172Yb
β-catenin	196624	147Sm

Supplementary Figure 4. In vivo therapeutic study and toxicity detection. (*A*) Sonogram of orthotopic tumor growth. High-frequency ultrasound was used to noninvasively monitor the growth of intrahepatic HCC. Tumor size was marked by circling the maximum diameter of the largest tumor area in the ultrasound plane. (*B*) Schematic of drug intervention protocol for tivantinib and the PD1 antibody in C57/BL6 mice. (*C*) Growth of orthotopic Hep1-6 tumors in tivantinib- and/or PD1 antibody-treated C57/BL6 mice. Tumors were measured at the indicated time points. (*D*) Survival of mice bearing Hep1-6 tumors after drug intervention with tivantinib and/or PD1 antibody. Significance was determined using log-rank test. (*E*) Immunohistochemical stains of PDL1, CD8, and granzyme B protein expression patterns in Hep1-6 cells. Scale bar, 50 μm. (*F*) Histogram showing mean immunohistochemistry score $\pm$ standard error of the mean in each group. $^{*}P < .05$; $^{**}P < .01$. (*G*) Growth of orthotopic MET KO Hep1-6 tumors in tivantinib- and/or PD1 antibody-treated C57/BL6 mice. Tumors were measured at the indicated time points. (*H*) Immunofluorescent staining of p-GSK3B (Y56) and PDL1 expression patterns in HCA-1 cells after drug intervention with capmatinib. (*I*) Curves showing body weight changes of mice during drug intervention. (*J*) Quantitative analysis of indicated biochemistry indices for liver and kidney function after the experiments. All error bars represent mean $\pm$ standard deviation. (*K*) Flow cytometric quantification of MET^{+} neutrophils in tumors of mice treated as indicated ($n = 6$; mean $\pm$ standard error of the mean). $^{**}P < .01$. (*L*) Immunofluorescent staining of MPO and MET expression patterns in HCA-1 tumors of mice treated as indicated (*M*) (*Left*) Western blot analysis of PDL1 protein and p-MET in lung cancer cell lines. (*Right*) Quantification of intensity of PDL1 protein and p-MET by a densitometer. ALT, alanine aminotransferase; BUN, serum urea nitrogen; DAPI, 4′,6-diamidino-2-phenylindole; IHC, immunohistochemistry; KO, knockout; MPO, myeloperoxidase; NS, not significant.

Supplemental Table 2. Components of GSK3B Complex Identified by Mass Spectrometry and Their Confidence Scores

Entry name	Coverage, %	Description	Score
G3P_HUMAN	82	Glyceraldehyde-3-phosphate dehydrogenase	3285
ANXA2_HUMAN	76	Annexin A2	2330
LDHB_HUMAN	58	L-lactate dehydrogenase B chain	1509
CAZA1_HUMAN	61	F-actin–capping protein subunit alpha-1	765
RLA0_HUMAN	45	60S acidic ribosomal protein P0	713
PP1B_HUMAN	59	Serine- and threonine-protein phosphatase PP1-beta catalytic subunit	674
LRC59_HUMAN	56	Leucine-rich repeat-containing protein 59	549
MDHM_HUMAN	53	Malate dehydrogenase, mitochondrial	516
MDHC_HUMAN	37	Malate dehydrogenase, cytoplasmic	495
NACA_HUMAN	36	Nascent polypeptide-associated complex subunit alpha	488
EF1D_HUMAN	30	Elongation factor 1-delta	481
PDLI1_HUMAN	51	PDZ and LIM domain protein 1	480
RL6_HUMAN	41	60S ribosomal protein L6	411
CNN2_HUMAN	32	Calponin-2	388
EF1A1_HUMAN	34	Elongation factor 1-alpha 1	369
ALDR_HUMAN	60	Aldose reductase	316
ROA2_HUMAN	28	Heterogeneous nuclear ribonucleoproteins A2/B1	314
PP2AA_HUMAN	39	Serine- and threonine-protein phosphatase 2A catalytic subunit alpha isoform	311
PDXK_HUMAN	33	Pyridoxal kinase	247
ENOA_HUMAN		Alpha-enolase	232
GALE_HUMAN	20	UDP-glucose 4-epimerase	223
RPR1B_HUMAN	40	Regulation of nuclear pre-mRNA domain-containing protein 1B	217
ALBU_HUMAN	11	Serum albumin	213
APEX1_HUMAN	42	DNA-(apurinic or apyrimidinic site) lyase	186
AIMP1_HUMAN	33	Aminoacyl tRNA synthetase complex-interacting multifunctional protein 1	183
SSRA_HUMAN	11	Translocon-associated protein subunit alpha	175
LMAN2_HUMAN	17	Vesicular integral-membrane protein VIP36	163
DHB4_HUMAN	8	Peroxisome multifunctional enzyme type 2	147
OTUB1_HUMAN	34	Ubiquitin thio-esterase OTUB1	122
PDIP2_HUMAN	20	Polymerase delta-interacting protein 2	118
HMOX2_HUMAN	31	Heme oxygenase 2	116
NDUA9_HUMAN	28	NADH dehydrogenase [ubiquinone] 1 alpha sub-complex subunit 9, mitochondrial	112
KPYM_HUMAN	74	Pyruvate kinase isozymes M1/M2	3356
TCPB_HUMAN	56	T-complex protein 1 subunit beta	1898
PDIA1_HUMAN	64	Protein disulfide-isomerase	1621
G6PI_HUMAN	66	Glucose-6-phosphate isomerase	1614
TCPD_HUMAN	56	T-complex protein 1 subunit delta	1422
TCPQ_HUMAN	65	T-complex protein 1 subunit theta	1409
TCPH_HUMAN	49	T-complex protein 1 subunit eta	1276
G6PD_HUMAN	63	Glucose-6-phosphate 1-dehydrogenase	998
CH60_HUMAN	39	60-kDa heat shock protein, mitochondrial	966
TCPA_HUMAN	57	T-complex protein 1 subunit alpha	939
IMDH2_HUMAN	46	Inosine-5′-monophosphate dehydrogenase 2	869
AL1A3_HUMAN	46	Aldehyde dehydrogenase family 1 member A3	854
PTBP1_HUMAN	42	Poly-pyrimidine tract-binding protein 1	756
PDIA3_HUMAN	45	Protein disulfide-isomerase A3	686
FKBP4_HUMAN	61	FK506-binding protein 4	625
CAP1_HUMAN	56	Adenylyl cyclase-associated protein 1	618
TCPZ_HUMAN	50	T-complex protein 1 subunit zeta	599
SERA_HUMAN	29	D-3-phosphoglycerate dehydrogenase	559
CPNE3_HUMAN	41	Copine-3	544
NP1L1_HUMAN	32	Nucleosome assembly protein 1-like 1	500
RCC2_HUMAN	40	Protein RCC2	491
TRXR1_HUMAN	29	Thioredoxin reductase 1, cytoplasmic	478
TBA1B_HUMAN	40	Tubulin alpha-1B chain	381
SYYC_HUMAN	39	Tyrosyl-tRNA synthetase, cytoplasmic	350
PRS4_HUMAN	31	26S protease regulatory subunit 4	345
UGDH_HUMAN	29	UDP-glucose 6-dehydrogenase	312
NONO_HUMAN	30	Non-POU domain-containing octamer-binding protein O	290
HNRPK_HUMAN	15	Heterogeneous nuclear ribonucleoprotein K	277
COPD_HUMAN	29	Coatomer subunit delta	259

Supplemental Table 2. Continued

Entry name	Coverage, %	Description	Score
PACN2_HUMAN	15	Protein kinase C and casein kinase substrate in neurons protein 2	222
PAK2_HUMAN	20	Serine–threonine–protein kinase PAK 2	203
HSP71_HUMAN	66	Heat shock 70-kDa protein 1	2989
HSP7C_HUMAN	58	Heat shock cognate 71-kDa protein	2639
GRP75_HUMAN	50	Stress-70 protein, mitochondrial	1913
LKHA4_HUMAN	49	Leukotriene A-4 hydrolase	1002
LMNB1_HUMAN	50	Lamin-B1	691
SYRC_HUMAN	31	Arginyl-tRNA synthetase, cytoplasmic	441
DDX5_HUMAN	29	Probable ATP-dependent RNA helicase DDX5	354
SYFB_HUMAN	25	Phenylalanyl-tRNA synthetase beta chain	327
ABCE1_HUMAN	30	ATP-binding cassette sub-family E member 1	304
CMC2_HUMAN	20	Calcium-binding mitochondrial carrier protein aralar2	265
FUBP1_HUMAN	23	Far upstream element-binding protein 1	260
TRI25_HUMAN	26	Tripartite motif-containing protein 25	239
RFA1_HUMAN	38	Replication protein A 70-kDa DNA-binding subunit	220
IF2B3_HUMAN	24	Insulin-like growth factor 2 mRNA-binding protein 3	209
TBA1A_HUMAN	25	Tubulin alpha-1A chain	174
AMPB_HUMAN	11	Aminopeptidase B	141
GRP78_HUMAN	59	78-kDa glucose-regulated protein	2917
MOES_HUMAN	58	Moesin	1846
PABP1_HUMAN	44	Polyadenylate-binding protein 1	1367
LMNA_HUMAN	57	Lamin-A/C	1322
HSP7C_HUMAN	37	Heat shock cognate 71-kDa protein	1320
CAN2_HUMAN	55	Calpain-2 catalytic subunit	1246
GUAA_HUMAN	62	GMP synthase (glutamine-hydrolyzing)	982
SRC8_HUMAN	33	Src substrate cortactin	957
PDIA4_HUMAN	44	Protein disulfide-isomerase A4	824
TRAP1_HUMAN	28	Heat shock protein 75-kDa, mitochondrial	765
DDX3X_HUMAN	31	ATP-dependent RNA helicase DDX3X	716
ECHA_HUMAN	42	Trifunctional enzyme subunit alpha, mitochondrial	653
K6PL_HUMAN	31	6-phosphofructokinase, liver type	642
CAN1_HUMAN	38	Calpain-1 catalytic subunit	559
TTL12_HUMAN	34	Tubulin–tyrosine ligase-like protein 12	558
ACSL3_HUMAN	25	Long-chain-fatty-acid–CoA ligase 3	530
SYG_HUMAN	33	Glycyl-tRNA synthetase	466
SEPT9_HUMAN	32	Septin-9	445
KPYM_HUMAN	34	Pyruvate kinase isozymes M1/M2	442
LAP2A_HUMAN	36	Lamina-associated polypeptide 2, isoform alpha	386
ALBU_HUMAN	12	Serum albumin	363
HNRPM_HUMAN	27	Heterogeneous nuclear ribonucleoprotein M	292
PYRG1_HUMAN	27	CTP synthase 1	289
GPDM_HUMAN	21	Glycerol-3-phosphate dehydrogenase, mitochondrial	239
VPS35_HUMAN	12	Vacuolar protein sorting-associated protein 35	225
GFPT1_HUMAN	14	Glucosamine–fructose-6-phosphate aminotransferase (isomerizing) 1	220
DC1I2_HUMAN	12	Cytoplasmic dynein 1 intermediate chain 2	217
SRP72_HUMAN	20	Signal recognition particle 72-kDa protein	206
DPP3_HUMAN	18	Dipeptidyl-peptidase 3	205
GLU2B_HUMAN	23	Glucosidase 2 subunit beta	201
ACPH_HUMAN	13	Acyl amino-acid–releasing enzyme	197
NDUS1_HUMAN	17	NADH-ubiquinone oxidoreductase 75-kDa subunit, mitochondrial	174
HS90B_HUMAN	63	Heat shock protein 90-beta	3824
ACTN1_HUMAN	71	Alpha-actinin-1	3652
EF2_HUMAN	59	Elongation factor 2	2026
ENPL_HUMAN	59	Endoplasmin	1951
TERA_HUMAN	56	Transitional endoplasmic reticulum ATPase	1461
IMB1_HUMAN	39	Importin subunit beta-1	993
GANAB_HUMAN	38	Neutral alpha-glucosidase AB	875
TFR1_HUMAN	29	Transferrin receptor protein 1	776
PYGL_HUMAN	33	Glycogen phosphorylase, liver form	644
PSA_HUMAN	29	Puromycin-sensitive aminopeptidase	551
SFPQ_HUMAN	21	Splicing factor, proline- and glutamine-rich	530

Supplemental Table 2. Continued

Entry name	Coverage, %	Description	Score
PSMD2_HUMAN	33	26S proteasome non-ATPase regulatory subunit 2	463
SSRP1_HUMAN	24	FACT complex subunit SSRP1	395
MCM3_HUMAN	24	DNA replication licensing factor MCM3	394
4F2_HUMAN	22	4F2 cell-surface antigen heavy chain	307
MCM6_HUMAN	14	DNA replication licensing factor MCM6	307
GELS_HUMAN	22	Gelsolin	305
AP2B1_HUMAN	11	AP-2 complex subunit beta-1	304
PDC6I_HUMAN	12	Programmed cell death 6-interacting protein	295
COPB2_HUMAN	16	Coatomer subunit beta′	292
COPG_HUMAN	14	Coatomer subunit gamma	292
CTND1_HUMAN	16	Catenin delta-1	280
HGFR_HUMAN	8	Hepatocyte growth factor receptor (HGFR)	276
SYMC_HUMAN	10	Methionyl-tRNA synthetase, cytoplasmic	252
NIBL1_HUMAN	16	Niban-like protein 1	226
RIR1_HUMAN	24	Ribonucleoside-diphosphate reductase large subunit	216
CSDE1_HUMAN	16	Cold shock domain-containing protein E1	210
NSUN2_HUMAN	12	tRNA (cytosine-5-)-methyltransferase NSUN2	205
CAPR1_HUMAN	10	Caprin-1	202
SYQ_HUMAN	11	Glutaminyl-tRNA synthetase	155
CTNB1_HUMAN	15	Catenin beta-1	151
MOGS_HUMAN	6	Mannosyl-oligosaccharide glucosidase	143
C1TC_HUMAN	63	C-1-tetrahydrofolate synthase, cytoplasmic	2726
VINC_HUMAN	56	Vinculin	2557
UBA1_HUMAN	39	Ubiquitin-like modifier-activating enzyme 1	1901
NUCL_HUMAN	41	Nucleolin	1807
XPO2_HUMAN	39	Exportin-2	1335
MYO1B_HUMAN	37	Myosin-Ib	1298
CTNA1_HUMAN	49	Catenin alpha-1	1236
IPO5_HUMAN	35	Importin-5	1211
ACLY_HUMAN	31	ATP-citrate synthase	944
HS105_HUMAN	39	Heat shock protein 105 kDa	928
PARP1_HUMAN	34	Poly(ADP-ribose) polymerase 1	883
EF2_HUMAN	39	Elongation factor 2	781
PUR2_HUMAN	32	Trifunctional purine biosynthetic protein adenosine-3	753
ACTN1_HUMAN	38	Alpha-actinin-1	734
SND1_HUMAN	39	Staphylococcal nuclease domain-containing protein 1	726
HNRPU_HUMAN	20	Heterogeneous nuclear ribonucleoprotein U	724
XPO1_HUMAN	29	Exportin-1	712
EIF3B_HUMAN	33	Eukaryotic translation initiation factor 3 subunit B	638
IPO7_HUMAN	27	Importin-7	604
PSA_HUMAN	28	Puromycin-sensitive aminopeptidase	576
TIF1B_HUMAN	25	Transcription intermediary factor 1-beta	542
ENPL_HUMAN	25	Endoplasmin	524
SYAC_HUMAN	24	Alanyl-tRNA synthetase, cytoplasmic	464
KINH_HUMAN	22	Kinesin-1 heavy chain	423
HS90B_HUMAN	20	Heat shock protein 90-beta	419
PSMD1_HUMAN	18	26S proteasome non-ATPase regulatory subunit 1	380
NALP2_HUMAN	17	NACHT, LRR and PYD domains containing protein 2	353
ITB1_HUMAN	19	Integrin beta-1	300
ICAL_HUMAN	31	Calpastatin	289
4F2_HUMAN	14	4F2 cell-surface antigen heavy chain	279
HXK1_HUMAN	23	Hexokinase-1	269
EIF3C_HUMAN	18	Eukaryotic translation initiation factor 3 subunit C	243
CAPR1_HUMAN	12	Caprin-1	243
AP1B1_HUMAN	15	AP-1 complex subunit beta-1	240
U5S1_HUMAN	22	116-kDa U5 small nuclear ribonucleoprotein component	236
SYIM_HUMAN	11	Isoleucyl-tRNA synthetase, mitochondrial	214
MVP_HUMAN	24	Major vault protein	195
ERAP1_HUMAN	12	Endoplasmic reticulum aminopeptidase 1	185
MYH9_HUMAN	68	Myosin-9	12446
FAS_HUMAN	52	Fatty acid synthase	4262

Supplemental Table 2. Continued

Entry name	Coverage, %	Description	Score
IQGA1_HUMAN	44	Ras GTPase-activating-like protein IQGAP1	2164
HGFR_HUMAN	38	Hepatocyte growth factor receptor (HGFR)	1479
MYOF_HUMAN	30	Myoferlin	1298
IF4G1_HUMAN	22	Eukaryotic translation initiation factor 4 gamma 1	943
FLNA_HUMAN	19	Filamin-A	900
PYR1_HUMAN	14	CAD protein	803
CLH1_HUMAN	10	Clathrin heavy chain 1	198
ALBU_HUMAN	10	Serum albumin	198
ZO1_HUMAN	6	Tight junction protein ZO-1	177
UBIQ_HUMAN	56	Ubiquitin	170